University of Illinois at Urbana-Champaign

Air Conditioning and Refrigeration Center A National Science Foundation/University Cooperative Research Center

Characterization of Acoustic Burst in Household Refrigerators

S. M. McLevige, J. S. Muka, and N. R. Miller

ACRC TR-200 March 2003

For additional information:

Air Conditioning and Refrigeration Center
University of Illinois
Mechanical & Industrial Engineering Dept.
1206 West Green Street
Urbana, IL 61801

(217) 333-3115

Prepared as part of ACRC Project #105
Sound Generation Mechanisms in Expansion Devices
N. R. Miller, Principal Investigator

The Air Conditioning and Refrigeration Center was founded in 1988 with a grant from the estate of Richard W. Kritzer, the founder of Peerless of America Inc. A State of Illinois Technology Challenge Grant helped build the laboratory facilities. The ACRC receives continuing support from the Richard W. Kritzer Endowment and the National Science Foundation. The following organizations have also become sponsors of the Center.

Alcan Aluminum Corporation
Amana Refrigeration, Inc.
Arçelik A. S.
Brazeway, Inc.
Carrier Corporation
Copeland Corporation
Dacor
Daikin Industries, Ltd.
Delphi Harrison Thermal Systems
Embraco S. A.
General Motors Corporation
Hill PHOENIX
Honeywell, Inc.
Hydro Aluminum Adrian, Inc.
Ingersoll-Rand Company
Kelon Electrical Holdings Co., Ltd.
Lennox International, Inc.
LG Electronics, Inc.
Modine Manufacturing Co.
Parker Hannifin Corporation
Peerless of America, Inc.
Samsung Electronics Co., Ltd.
Tecumseh Products Company
The Trane Company
Valeo, Inc.
Visteon Automotive Systems
Wieland-Werke, AG
Wolverine Tube, Inc.

For additional information:

Air Conditioning & Refrigeration Center
Mechanical & Industrial Engineering Dept.
University of Illinois
1206 West Green Street
Urbana, IL 61801

217 333 3115

Characterization of Acoustic Burst in Household Refrigerators

S. M. McLevige, J. S. Muka, N. R. Miller

University of Illinois at Champaign/Urbana
Mechanical and Industrial Engineering Department
Air Conditioning and Refrigeration Center

ABSTRACT

The purpose of this work was to investigate and characterize the acoustic burst ("popping") phenomenon occurring in household refrigerators shortly after compressor start-up. An experimental investigation began with a household refrigerator that regularly experienced acoustic bursts and was followed by construction of an apparatus that allowed control of system conditions. It was found that refrigerant vapor must be present in the capillary tube and suction line temperature must significantly drop in order for the occurrence of acoustic bursts. This suggests that the root cause of acoustic bursts is condensation induced shock. Using simple instrumentation and model predictions to characterize the acoustic burst phenomenon, it was found that acoustic bursts begin to occur at Jakob numbers approximately around one and the Jakob number can be used to characterize acoustic burst magnitude. Heat exchanger orientation and compressor oil addition (0.5% by weight) do not have a significant effect on acoustic bursts.

Keywords: Acoustic burst; Popping; Domestic refrigerators; Condensation induced shock; Jakob number

INTRODUCTION

For many years, manufacturers of household refrigerators have been investigating an acoustic burst or "popping" that occurs shortly into the compressor on cycle. At compressor start-up, a redistribution of refrigerant takes place causing large pressure and temperature transients in the system [1, 2, 3]. Figure 1 depicts how the acoustic burst event during the compressor start-up cycle of a household refrigerator could occur.

Initial Experimentation

In a standard household refrigerator, refrigerant pools in the evaporator during the compressor off cycle. Vapor exists in all components outside the freezer compartment. At compressor start-up, the evaporator empties the excess refrigerant through the suction line, the pressure in the condenser rises, and refrigerant starts to pool in the condenser. Until the condenser is able to output a sufficient amount of liquid, only vapor enters the capillary tube. During initial experiments on a domestic refrigerator (details regarding test procedures and facilities are provided in Appendix A), the suction line heat exchanger temperature dropped to nearly the evaporator temperature (Figure 2). The temperature along the suction line heat exchanger remained at approximately the evaporator temperature until the refrigerant redistributed and liquid began to enter the capillary tube while vapor began to enter the suction line. Most importantly, the acoustic burst phenomenon occurred when the suction line temperature dropped. The surface temperature of the suction line does not begin to increase until after the acoustic burst event has ended (approximately 50 seconds after the compressor turns on).

Shortly after the beginning of the compressor on cycle, the vapor flow transitions to liquid flow at the capillary tube inlet. At this point, vapor bubbles entrained by cold sub-cooled liquid could possibly enter the capillary tube. The measured temperature and saturation temperature (based on measured pressure) in the filter dryer, which corresponds to the capillary inlet conditions, are shown in Figure 3. While the compressor is off, superheated vapor filled the filter dryer. After the compressor turns on, the pressure (and thus the saturation temperature) began to rise and two-phase liquid entered the filter dryer. Eventually, the condenser filled with liquid and therefore only liquid enters the filter dryer. In effect, the capillary inlet is sealed by liquid. As liquid covers the capillary tube inlet, the filter dryer pressure increases until the equilibrium pressure is reached. Through the use of a glass filter dryer, vortex formation was observed as the liquid level neared the capillary tube inlet. In the observed domestic refrigerator, the acoustic burst phenomenon occurred only during vortex formation.

Condensation Induced Shock

Occurrence of acoustic bursts only during the drop in temperature of the suction line and vortex formation at the capillary tube inlet (possibly leading to vapor bubble ingestion) suggests conditions that could support condensation induced shock. Condensation induced shock (CIS) occurs when a bubble of vapor at saturation temperature is trapped in saturated liquid and then the liquid is cooled to a temperature significantly below its saturation temperature. The vapor bubble collapses suddenly producing a shock wave in the liquid medium. A large body of work does not exist for condensation induced shock in refrigeration systems; however, Jacobi and Shelton investigated condensation induced shock in ammonia systems [4, 5].

Jakob Number

The strength of an acoustic burst event is dependent upon a number of properties, which include fluid properties and speed of bubble collapse. For a given set of fluid properties, the speed of bubble collapse is related to heat transfer with the collapse rate increasing with increased heat transfer [6, 7, 8, 9, 10]. When heat transfer is large enough, the upper limit of the collapse rate is reached and the bubble collapses near the fluid inertial limit. Before the inertial limit is reached the speed of bubble collapse is related to the heat transfer between the vapor bubble and the surrounding liquid. The possibility of acoustic burst by condensation induced shock suggests that such an event can be characterized by examining the difference between the saturation temperature and sub-cooled temperature of the liquid medium; consequently, a dimensionless combination of variables called the Jakob number (Ja) [5] can be used. The Jakob number is defined as:

$$Ja = \frac{\rho_L c_L (T_S - T_L)}{\rho_G h_{FG}} \quad (1)$$

where:

$\rho_L \equiv$ density of liquid

$\rho_G \equiv$ density of gas

$h_{FG} \equiv$ latent heat of vaporization (214.96kJ/kg)

$C_L \equiv$ specific heat of liquid

$T_S \equiv$ saturation temperature

$T_L \equiv$ temperature of liquid

The Jakob number gives the ratio of the rate that heat can leave a vapor bubble to the rate that heat needs to be rejected in order to condense the vapor bubble. A higher Jakob number corresponds to a faster condensation rate. Jakob numbers above 1 correspond to the case where heat is leaving the vapor bubble at a rate faster than the rate heat needs to be rejected in order to condense the vapor bubble.

RESULTS AND DISCUSSION

Observed Household Refrigerator

In addition to the initial experiments conducted on a household refrigerator, the effect of suction line temperature and vortex formation at the capillary inlet on the incidence of acoustic bursts was further investigated.

Suction Line Temperature

To determine the relationship between the drop in temperature of the suction line and the acoustic burst phenomenon, the temperature of the suction line was increased using a warming tube (see Appendix A). Figures 4 and 5 show temperature profiles during the compressor on cycle with and without warming of the suction line heat exchanger, respectively. In the case where the suction line heat exchanger was warmed, the acoustic burst event did not occur. When the suction line heat exchanger was not warmed, the acoustic burst occurred within the expected time frame. This suggests that the acoustic burst phenomenon is dependent on the drop in temperature of the suction line.

Capillary Inlet Conditions and Vortex Formation

To determine the relationship between vortex formation at the capillary inlet inside the filter dryer and the acoustic burst phenomenon, the filter dryer orientation was changed from vertical to horizontal (with respect to the ground). Acoustic bursts occur when the filter dryer was oriented vertically. However when the filter dryer was oriented horizontally, the acoustic burst phenomenon did not occur. Figures 6 and 7 show the temperature profiles of the system with vertical filter dryer and horizontal filter dryer orientation, respectively. Changing the orientation of the filter dryer does not change the temperature profiles. Changing the filter dryer orientation from vertical to horizontal probably stops vortex formation at the capillary tube inlet. This suggests that the acoustic burst phenomenon is dependent on the formation of a vortex at the capillary tube inlet.

Acoustic Burst Characterization

In order to investigate the magnitude of the Jakob number when the acoustic burst event occurs in the observed household refrigerator, filter dryer pressures and suction line temperatures were recorded during the acoustic burst time frame. Using filter dryer pressure and suction line temperature, a model (see Appendix B for model description and validation) was used to predict the Jakob number of the refrigerant in the capillary tube. Figure 8 shows that the maximum Jakob number during the acoustic burst phenomenon is approximately 3.7.

Experimental Apparatus

To study the acoustic burst phenomenon in a controlled manner, an experimental apparatus that approximates the suction line heat exchanger of a household refrigeration system was fabricated (details regarding the experimental apparatus are provided in Appendix A). In a typical household refrigerator, the suction line heat exchanger consists of a copper capillary tube located adjacent to a copper suction line. In the experimental

apparatus, the simulated suction line heat exchanger consists of a copper capillary tube located inside a coolant tube forming a counter flow heat exchanger.

Vortex Behavior

A vortex formed at the capillary tube inlet of the experimental apparatus when two-phase refrigerant was present. Using the needle valves on the simulated filter dryer controlled the submergence level of the capillary tube inlet. Increasing vapor refrigerant flow decreases capillary tube inlet submergence, while increasing liquid refrigerant flow increases capillary tube inlet submergence. As shown in Figure 9 (taken from [11]), the vortex flow at the capillary tube inlet changes with capillary tube inlet submergence level. Type A represents a large vortex that dips into the capillary tube. As the submergence level was raised to type B, the vortex narrowed. In type C, a dimple depression appears on the surface of the liquid. At random times a vapor bubble would break away from the dimple and enter the capillary tube. In type D, the submergence level has increased to a point where no vortex forms and only liquid appears to enter the capillary tube. The type C vortex is similar to the "conically depressed surface with entrainment of relatively large round bubbles" as described by Takahashi [11]. Acoustic burst events were only detected when a type C vortex formed at the simulated capillary tube inlet (and the chilling fluid was sufficiently cold). This suggests that the ingestion of a vapor bubble into the capillary tube is necessary for the occurrence of an acoustic burst event.

Acoustic Burst Characterization

Approximating the typical filter dryer pressure seen in the observed household refrigerator, the primary experimental apparatus tests were performed at an upstream pressure of 689.5kPa. By measuring the RMS value of the capillary flow noise with a digital multi-meter, monitoring the acoustic burst magnitude as measured by an accelerometer with an oscilloscope, and assuming capillary flow noise with a normal distribution, the number of standard deviations of a particular acoustic burst (burst magnitude divided by the RMS value of the flow noise) can be determined. Figure 10 shows the Jakob number characterization of refrigerant flow through the simulated suction line heat exchanger capillary tube for both pure refrigerant (R134a) and a refrigerant-oil mixture (99.5% R134a, 0.5% RL10H by weight) using the number of standard deviations of a particular acoustic burst (recorded at a particular cooling fluid temperature) to provide a quantitative measure for the differentiation of acoustic burst magnitude regimes.

Three acoustic burst regimes are denoted in Figure 10: "no burst", "weak/no burst", and "strong burst". In the no burst regime, the acoustic burst standard deviations is less than or equal to 3. Approximately 99% of standard flow noise is contained within this regime; however, it is not possible to discern between white flow noise and an acoustic burst. In the weak/no burst regime, the acoustic burst standard deviation is between 3 and 5. Approximately 100% of flow noise is contained within this regime. Acoustic bursts seen in this region have a small chance of being standard flow noise. In the strong burst regime, the burst magnitude standard deviation is above 5. The magnitude of the acoustic bursts found in this regime precludes almost any possibility of being within the distribution of standard flow noise.

According to model predictions at 689.5kP, the transition from the no burst regime to the weak/no burst regime occurs at a maximum Jakob number (of the refrigerant flow through the capillary tube in the simulated

suction line heat exchanger) of approximately 1.0 and the transition from the weak/no burst regime to the strong burst regime occurs at a maximum Jakob number of approximately 1.7.

During normal operation of a household refrigerator, the refrigerant line is mixed with compressor oil; therefore, tests were performed using both a pure refrigerant and a refrigerant-oil mixture. Figure 10 shows no significant difference between the acoustic burst behavior of the pure refrigerant and the refrigerant-oil mixture.

In addition to the 689.5kPa tests, the experimental apparatus was used to conduct tests at 551.6kPa and 827.4kPa using pure refrigerant. Figure 11 shows the model reconstruction of the Jakob number (as a function of simulated suction line heat exchanger position) calculated at the no burst to weak/no burst regime and weak/no burst regime to strong burst regime cooling fluid transition temperatures (as determined from experimental observation). According to model predictions at 551.6kPa, the transition from the no burst regime to the weak/no burst regime occurs at a maximum Jakob number of approximately 0.8 and the transition from the weak/no burst regime to the strong burst regime occurs at a maximum Jakob number of approximately 2.3. According to model predictions at 827.4kPa, the transition from the no burst regime to the weak/no burst regime occurs at a maximum Jakob number of approximately 1.3 and the transition from the weak/no burst regime to the strong burst regime occurs at a maximum Jakob number of approximately 2.0.

Examining the 551.6, 689.5, and 827.4kPa data, weak bursts begin to occur at a Jakob number of approximately 1. As the Jakob number increases, the magnitude of the acoustic burst transitions to the strong burst regime. The strong burst regime is entered at a Jakob number approximately between 1.7 and 2.3.

In addition to investigating the effect of oil contamination on acoustic burst, the effect of heat exchanger orientation on the Jakob number profile was investigated. Figure 12 shows the model predictions for varying heat exchanger orientation from the horizontal position to 90° vertical-up (refrigerant flow opposes gravity) and 90° vertical-down (refrigerant flow aided by gravity). For this experimental apparatus, the heat exchanger orientation has a small effect on the Jakob number profile and therefore a small effect on the acoustic burst phenomenon. Experimental results support the model predictions.

CONCLUSIONS

A household refrigerator that regularly demonstrated the acoustic burst phenomenon and an apparatus that allowed control of system conditions were experimentally investigated. Using simple temperature and pressure measurements, characterization of the acoustic burst occurring in some household refrigerators was performed. Major findings are:

(1) Experimental results support the hypothesis that the acoustic burst seen in the observed refrigeration system is due to condensation induced shock. The acoustic burst event shows a dependence on a drop in temperature of the suction line and vortex formation leading to vapor bubble ingestion at the capillary tube inlet.

(2) Weak acoustic bursts or bursts not located outside the standard flow noise to a high degree of certainty begin to occur in the experimental apparatus at a Jakob number of approximately 1. Since Jakob numbers above 1 correspond to the case where heat is leaving the vapor bubble at a rate faster than the rate heat needs to be rejected in order to condense the vapor bubble, the experimental data and model predictions agree with the basic definition of the Jakob number.

Strong acoustic bursts or bursts significantly above the standard flow noise (greater than 5σ) begin to occur in the experimental apparatus at Jakob numbers between 1.7 and 2.3.

(3) The maximum Jakob number occurring at the same time that a strong acoustic burst was reported to occur in the observed refrigeration system is 3.7. According to characterization of the acoustic bursts regimes in the experimental apparatus, a Jakob number of 3.7 supports the supposition of a strong acoustic burst in the observed household refrigerator; however, further experimentation is needed to investigate the relation of the classification of acoustic burst regimes in the observed household refrigerator and the classification of acoustic burst regimes in the experimental apparatus.

(4) Addition of compressor oil to the refrigerant (0.5% by weight) and heat exchanger orientation do not have a significant effect on the acoustic burst phenomenon.

ACKNOWLEDGEMENTS

The authors would like to thank the Air Conditioning and Refrigeration Center at the University of Illinois at Urbana-Champaign for their support of the present work.

APPENDIX A: TEST FACILITIES AND PROCEDURES

Observed Refrigeration System

A household refrigerator was instrumented to identify the operating conditions under which the acoustic burst phenomenon occurs. A schematic of the refrigerator instrumentation is shown in Figure 13. Table 1 contains a list of sensors installed on the refrigeration line.

The capillary tube is made of copper and has an inner diameter of 0.091cm and an outer diameter of 0.223cm. The suction line is made of copper and has a cross-sectional area approximately 48 times as large as the cross-sectional area of the capillary tube.

In order to test the importance of the drop in temperature of the suction line to the occurrence of the acoustic burst phenomenon, a modification was made to the original refrigeration line. As shown in Figure 14, water (at 22°C) was pumped through a copper tube clamped to the suction line.

Experimental Apparatus

An experimental apparatus was designed to approximate the suction line heat exchanger of a typical household refrigerator (Figure 15). The simulated suction line heat exchanger consisted of a copper capillary tube located inside a coolant tube forming a counter flow heat exchanger. Cooling fluid (a mixture of potassium formate and water) is pumped through the outer coolant tube at approximately 0.4kg/s. The temperature of the cooling fluid is controlled by a chiller unit. The apparatus uses a 133.4N tank of R134a refrigerant in a heated bath to provide a source of refrigerant at the desired temperature and pressure. Needle valves are used to control vortex formation in the filter dryer and hence the ingestion of refrigerant vapor bubbles into the simulated suction line heat exchanger.

Thermocouples (T type) were used to monitor the temperature of the refrigerant and the cooling fluid at the inlet and outlet of the simulated suction line heat exchanger. Insulated surface thermocouples (T type) were used to measure inlet and outlet refrigerant temperatures. According to Bullard [12], proper insulation of the surface mounted thermocouple effectively drives the thermocouple temperature measurement to within the margin of error of the thermocouple instrumentation. The thermocouple used to measure inlet refrigerant temperature was located 10.16cm from the heat exchanger inlet and the thermocouple (T type) used to measure outlet refrigerant temperature was located 10.16cm from the heat exchanger outlet. Immersed thermocouples (T type) were located at the inlet and outlet of the cooling fluid. An accelerometer (located 8.89cm from the capillary tube exit) was used to detect the magnitude of the acoustic burst relative to the normal refrigerant flow noise.

Upstream (simulated filter dryer) pressures of 551.6, 689.5, and 827.4kPa were maintained while varying the cooling fluid temperature. Tests began with the cooling fluid temperature at -20°C (the acoustic burst event is easily detected for all upstream pressures at this temperature). The cooling fluid temperature was allowed to warm-up until the acoustic burst event was no longer detected.

For further details on test facilities and procedures, refer to [13].

APPENDIX B: CAPILLARY TUBE MODEL

Model Description

In order to predict the temperature distribution of the refrigerant along the length of the capillary tube, a simple model of the experimental apparatus counter flow heat exchanger was developed using Engineering Equation Solver (EES) software. The major model assumptions for both the refrigerant and cooling fluid flow are one dimensional incompressible fluid flow, constant head loss along the capillary tube neglecting losses due to gravity, and fully developed turbulent flow using the Gnielinski approximation for the Nusselt number [14]. The model inputs are refrigerant inlet pressure, mean cooling fluid temperature, and heat exchanger position. The primary model outputs are refrigerant temperature and Jakob number of the capillary tube refrigerant flow.

Along with the major model assumptions, the variation of refrigerant temperature in the radial direction is considered negligible. In addition, the model uses experimentally determined values in order to predict capillary tube head loss, refrigerant inlet temperature, and mean refrigerant temperature. The head loss values were determined as a function of measured inlet pressure (assuming atmospheric outlet conditions). The refrigerant inlet temperatures were experimentally determined as a function of cooling fluid temperature and refrigerant inlet pressure. The mean refrigerant temperature (used to evaluate refrigerant properties) was approximated as a function of cooling fluid temperature, refrigerant inlet pressure, and heat exchanger position. Assuming that the refrigerant is a pure saturated liquid with 100% quality, the refrigerant density, viscosity, Prandtl number, and conductivity were considered functions of mean refrigerant temperature.

For turbulent flow in a pipe, the friction factor varies according the Colebrook equation:

$$\frac{1}{\sqrt{f}} = -2\log\left(\frac{\varepsilon/d}{3.7} + \frac{2.5}{Re\sqrt{f}}\right) \tag{2}$$

where:

f ≡ friction factor

ε ≡ surface roughness

d ≡ diameter

Re ≡ Reynolds number

$$V = \left(\frac{2gh}{K_{in} + K_{out} + \frac{fL}{d}}\right)^{\frac{1}{2}} \tag{3}$$

Given a capillary tube surface roughness of 1.524e-6m [15], the average refrigerant velocity can be determined:

where:

V ≡ average velocity

g ≡ acceleration due to gravity

h ≡ head loss

K_{in} ≡ resistance coefficient of tube inlet

K_{out} ≡ resistance coefficient of tube outlet

L ≡ tube length

Given inlet and outlet capillary tube resistance of 1 [15], the refrigerant mass flow rate and the refrigerant Reynolds number can be calculated. Using the Gnielinski approximation, the Nusselt number corresponding to a turbulent flow in a circular tube is:

$$Nu = \left(\frac{\left(\frac{f}{8}\right)(Re-1000)Pr}{1+12.7(f/8)^{1/2}\left(Pr^{2/3}-1\right)} \right) \tag{4}$$

where:

Pr ≡ Prandtl number

Given that the Prandtl number can be determined from the mean refrigerant temperature, the Nusselt number is known and the refrigerant convection coefficient can be calculated.

Since the temperature of the cooling fluid is constant along the entire length of the heat exchanger (as per immersed thermocouple data), determination of the cooling fluid properties is straightforward. The properties of the cooling fluid were approximated with water properties. The flow rate, mean pressure, and mean temperature (model input) are known a priori for a particular model run. The Prandtl number and thermal conductivity can be determined using the mean pressure and temperature. As in the determination of the Nusselt number of the refrigerant flow, the Nusselt number for the cooling fluid was determined using the Gnielinski approximation and hence the cooling fluid convection coefficient can be calculated. Since the surface roughness effects of the cooling fluid tube are negligible, a smooth tube approximation of the friction factor was used for the cooling fluid flow:

$$f = (0.79\ln(Re) - 1.64)^{-2} \tag{5}$$

After using standard methods to calculate the overall convection coefficient, the NTU method [16] was used to calculate the outlet temperature of the refrigerant. Note that the specific heat of the refrigerant was considered to be a function of mean refrigerant temperature, while the specific heat of the cooling fluid was calculated as a function of mean cooling fluid temperature and pressure.

Once the outlet temperature of the refrigerant is known, the Jakob number can be calculated for a particular heat exchanger position as per equation (1). Liquid density and liquid specific heat were considered weak functions of pressure; therefore, the refrigerant liquid density and the refrigerant specific heat were calculated as functions of only refrigerant outlet temperature. In addition, the saturated vapor density is calculated at the saturation pressure and the saturation temperature is calculated at the refrigerant outlet pressure.

Model Validation

To determine the validity of the turbulent refrigerant flow assumption, the model was tested for both turbulent and laminar refrigerant flow through the capillary tube. Figure 16 shows model temperature predictions along with experimentally obtained inlet and outlet capillary tube refrigerant temperatures for an inlet pressure of 689.5kPa; consequently, the fully developed turbulent flow assumption approximates the capillary tube outlet temperatures more closely than the laminar flow assumption. Assuming fully developed turbulent flow, model predictions and experimentally obtained temperature data show acceptable agreement. Model assumptions, location of the thermocouples, and/or thermocouple accuracy may contribute to the difference in predicted and experimental refrigerant outlet temperatures. Given a particular upstream pressure and a cooling fluid temperature, the model was used to predict the Jakob number as a function of heat exchanger position.

REFERENCES

[1] Wang, J. and Wu, Y. “Start-up and shut-down operation in a reciprocating compressor refrigeration system with capillary tubes.” International Journal of Refrigeration, 1990; 13[3]; 187-190.

[2] Rubas, P. J. and Bullard, C. W. “Factors contributing to refrigerator cycling losses.” International Journal of Refrigeration, 1995; 18[3]; 168-176.

[3] Coulter, W. H. and Bullard, C. W. “An experimental analysis of cycling losses in domestic refrigerators-freezers.” ASHRAE Transactions, 1997; 103[1]; 587-596.

[4] Jacobi, A. M. and Shelton, J. “A fundamental study of refrigerant-line transients: part 1 – description of the problem and survey of relevant literature.” ASHRAE Transaction, 1997; 103[1]; 1-12.

[5] Shelton, J. C. and A. M. Jacobi, “A fundamental study of refrigerant line transients.” ACRC CR-04, University of Illinois at Urbana-Champaign, 1995.

[6] Rayleigh, Lord. “On the pressure developed in a liquid during the collapse of a spherical cavity.” Philosophical Magazine, 1917; 34; 94-98.

[7] Zwick, S. A. and Plesset, M. S. “On the dynamics of small vapor bubbles in liquids.” Journal of Mathematics and Physics, 1955; 33; 308-329.

[8] Hunter, C. “On the collapse of an empty cavity in water.” Journal of Fluid Mechanics, 1960; 8; 241-262.

[9] Florschuetz, L. W. and Chao, B. T. “On the mechanics of vapor bubble collapse.” Journal of Heat Transfer, 1965; 87[2]; 202-220.

[10] Wittke, D. D. and Chao, B. T. “Collapse of vapor bubbles with translatory motion.” Journal of Heat Transfer, 1967; 89[1]; 17-24.

[11] Takahashi, M., InOue, A., and Aritomi, M. “Gas entrainment at free surface of liquid.” Journal of Nuclear Science, 1988; 25[2]; 131-142.

[12] Personal Correspondence with Professor C. Bullard, University of Illinois Champaign-Urbana.

[13] McLevige, S. M. and Miller, N. R. “Experimental investigation of the source of acoustic bursts produced by household refrigerators.” Master Thesis, University of Illinois, 2001.

[14] Incropera, F. P, and DeWitt D. P. Fundamental of Heat and Mass Transfer. John Wiley and Sons, Inc, 1990; 497.

[15] Marks’ Standard Handbook for Mechanical Engineers, 10th Edition, McGraw-Hill, 1996; 3-47 to 3-51.

[16] Incropera, F. P, and DeWitt D. P. Fundamental of Heat and Mass Transfer. John Wiley and Sons, Inc, 1990; 639-672.

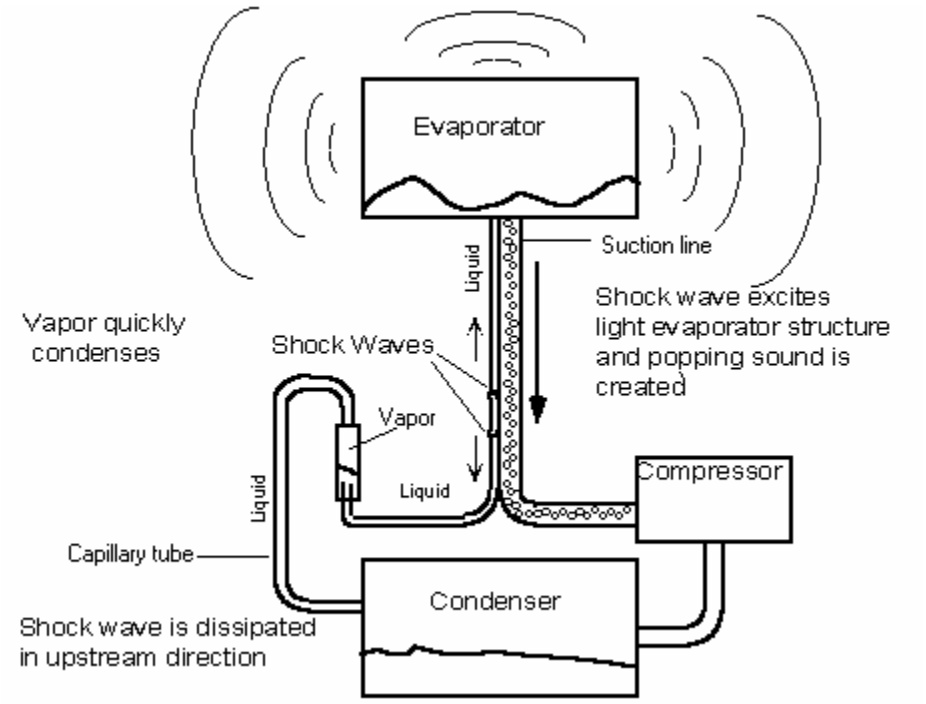

Figure 1 – Acoustic Burst Schematic

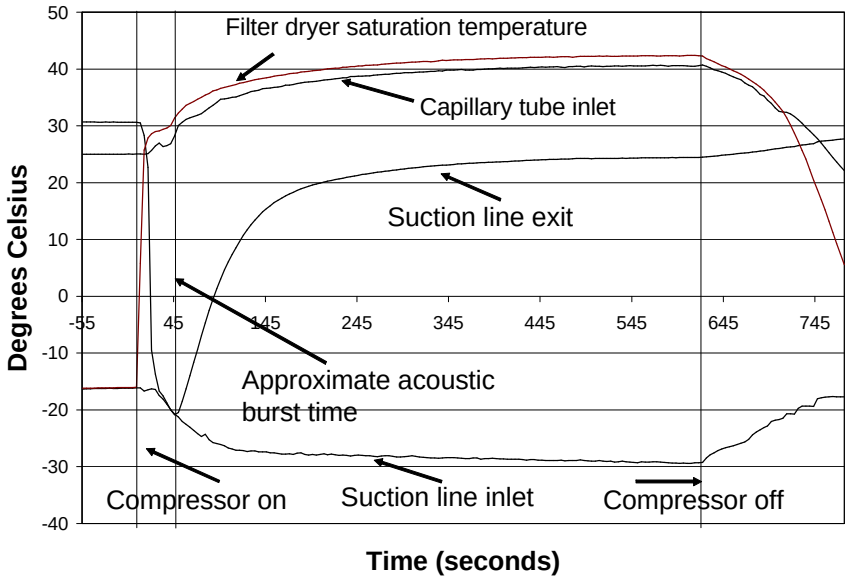

Figure 2 – Compressor Cycle Temperature Profile

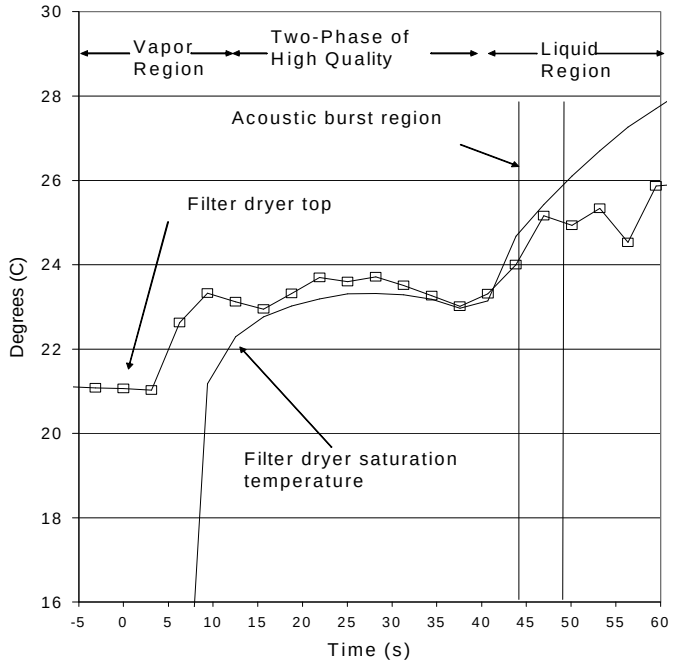

Figure 3 – Capillary Tube Inlet Conditions

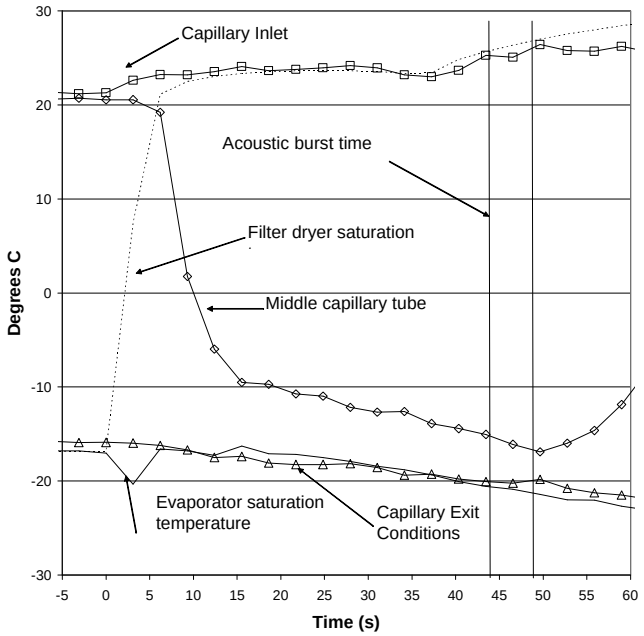

Figure 4 – No Warming of Suction Line Heat Exchanger (Acoustic Burst)

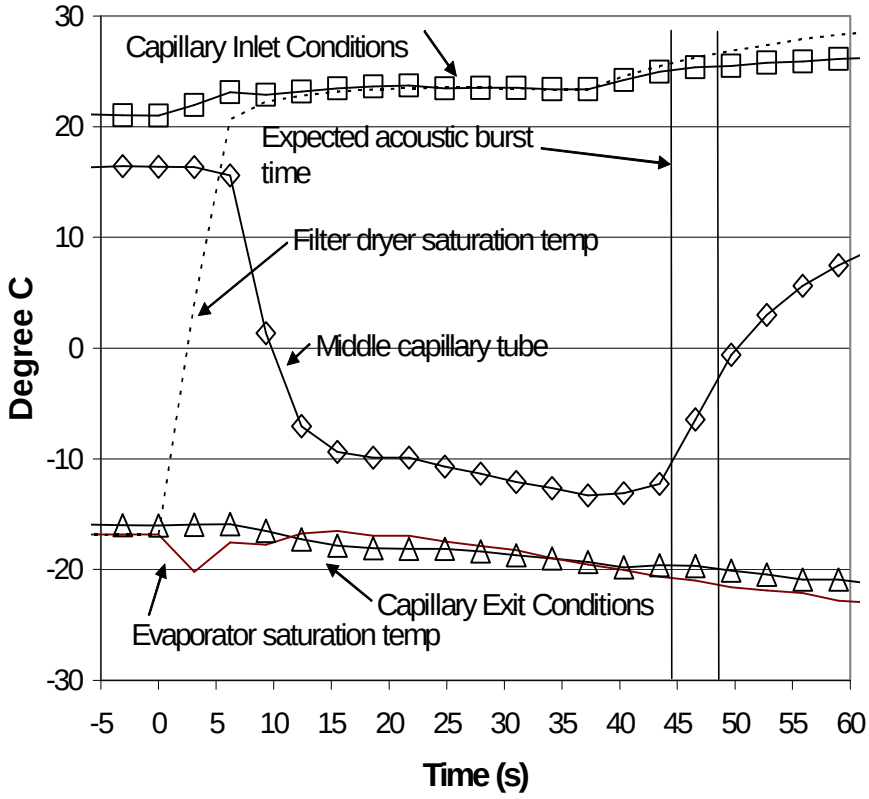

Figure 5 – Warming of Suction Line Heat Exchanger (No Acoustic Burst)

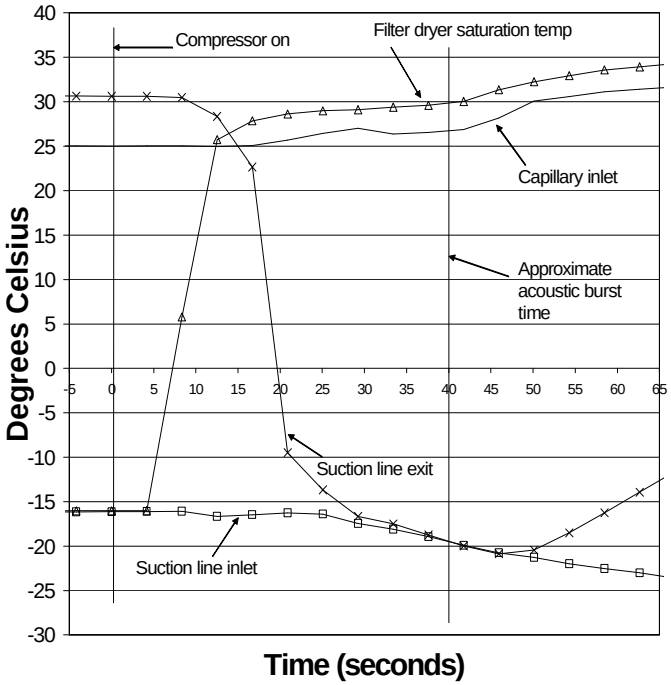

Figure – 6 Vertical Filter Dryer

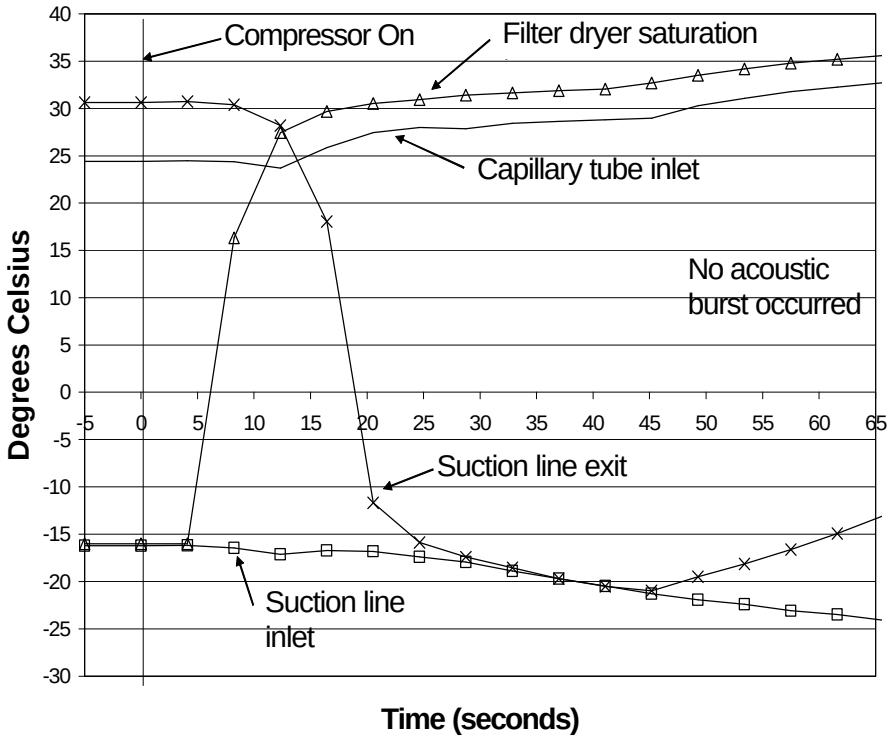

Figure 7 – Horizontal Filter Dryer

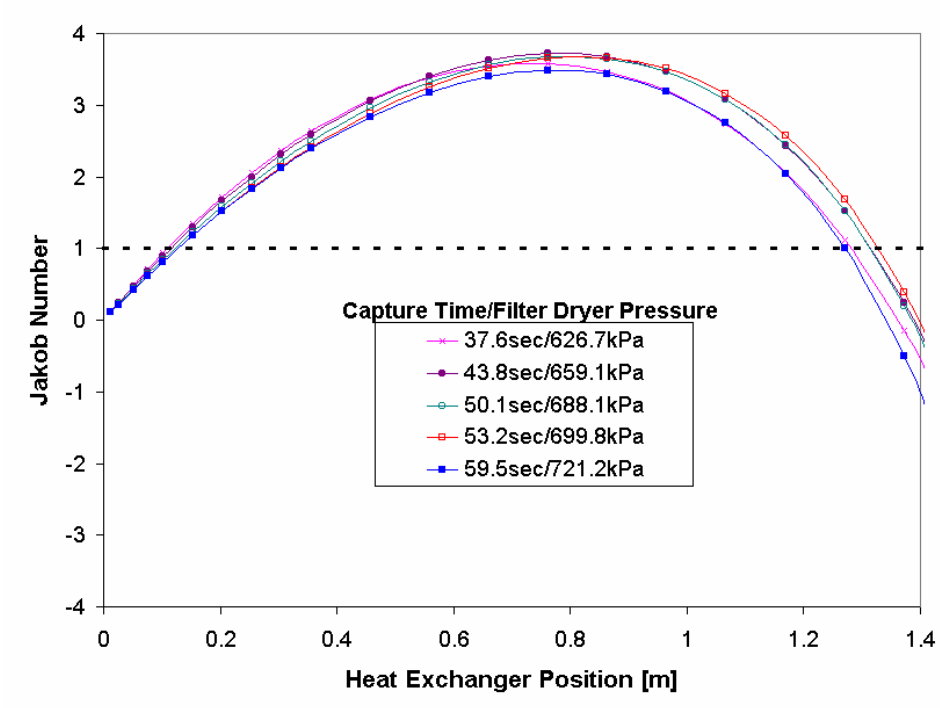

Figure 8 – Original Refrigeration System during Acoustic Burst

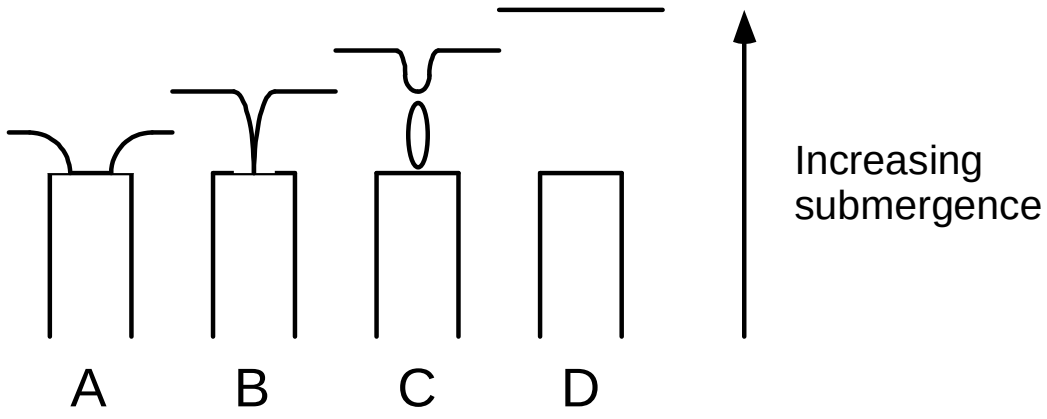

Figure 9 – Vortex Dependence on Submergence [11]

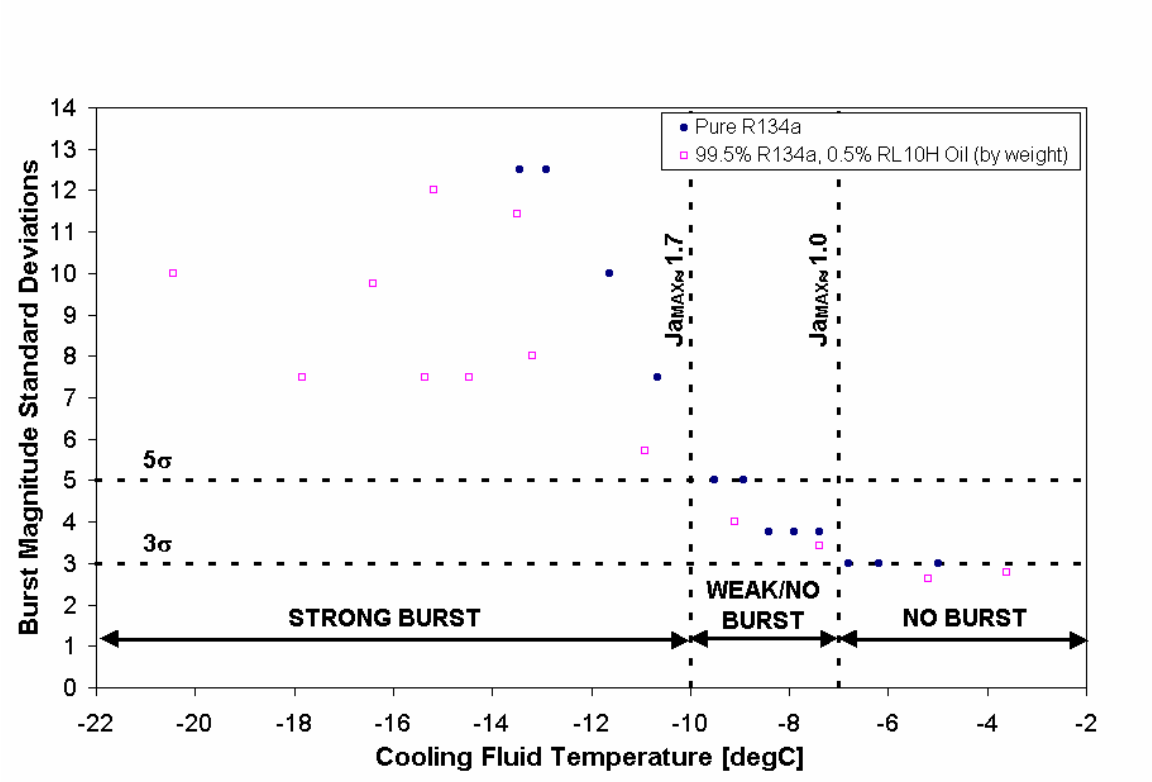

Figure 10 – Experimental Apparatus Refrigerant-Oil Mixture Tests at 689.5kPa: Burst Magnitude Standard Deviations vs. Cooling Fluid Temperature [degC]

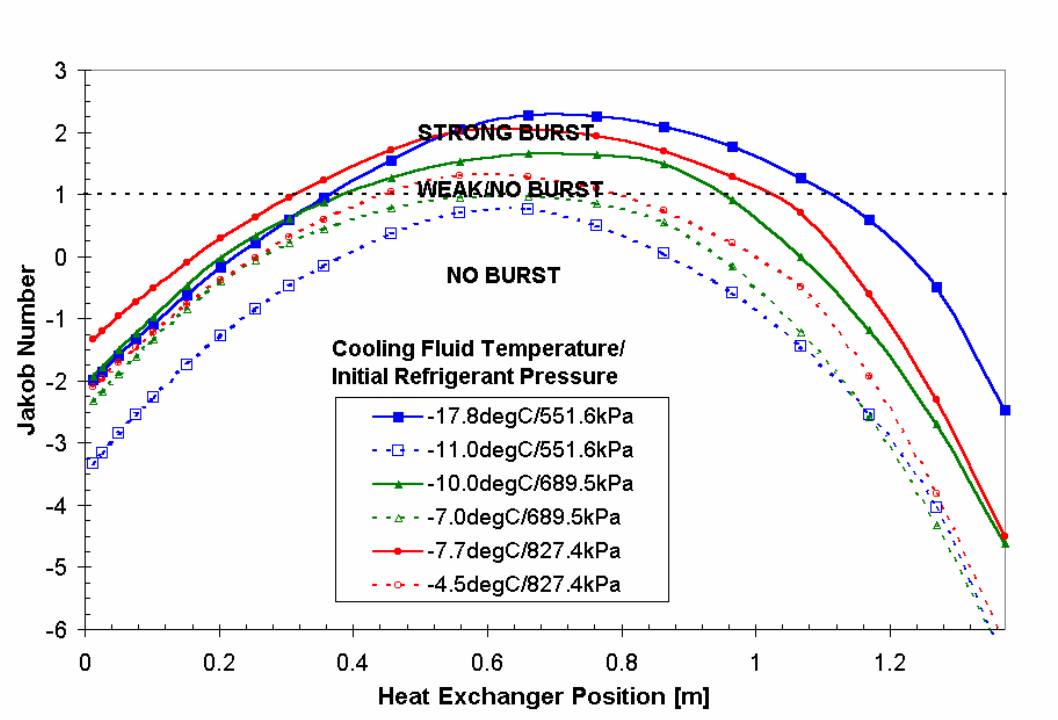

Figure 11 – Characterization of Experimental Apparatus

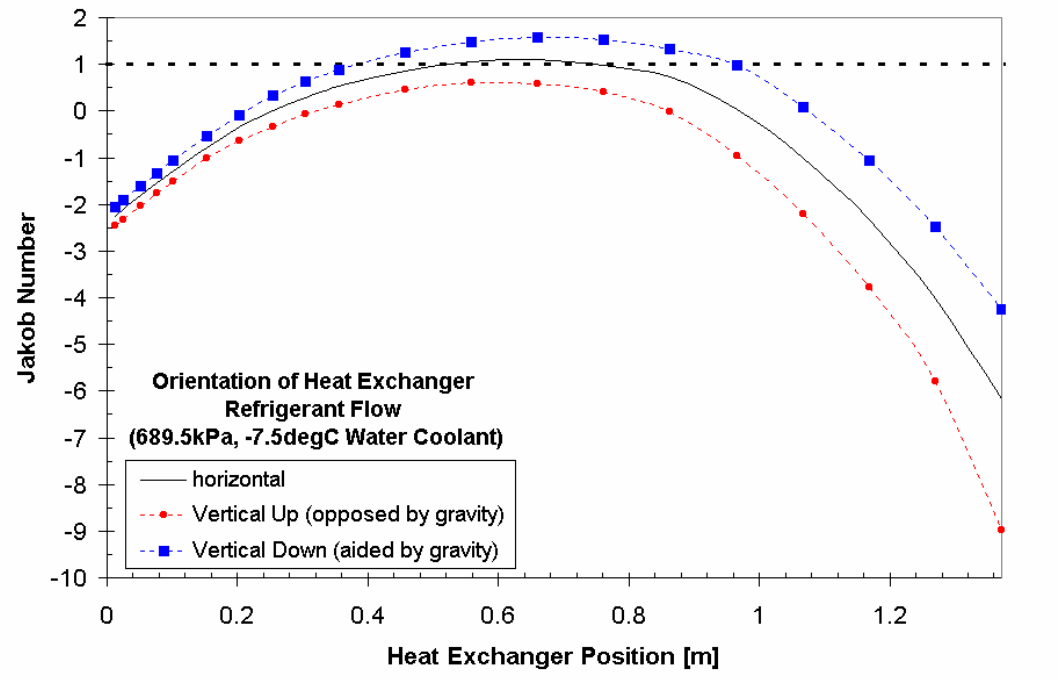

Figure 12 – Effect of Heat Exchanger Orientation

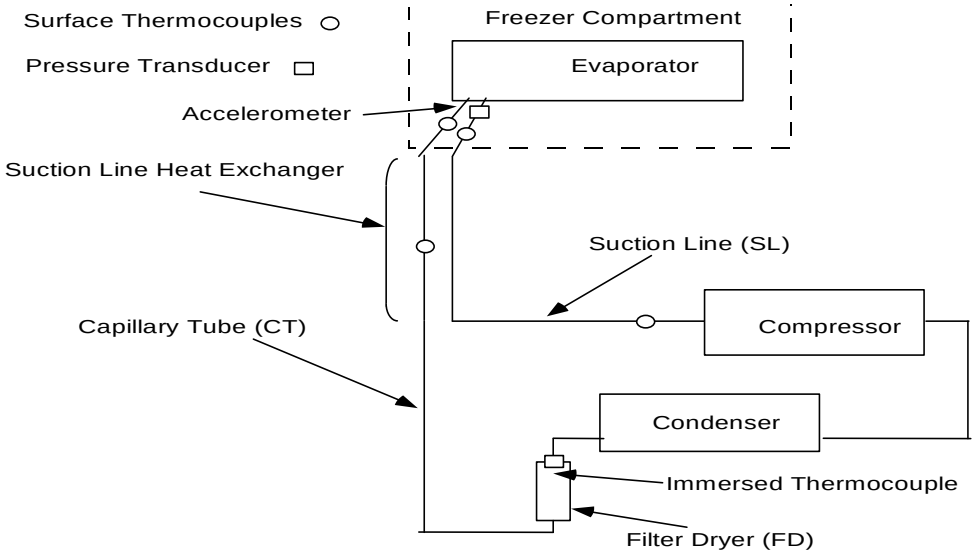

Figure 13 – Household Refrigeration Line Test Schematic

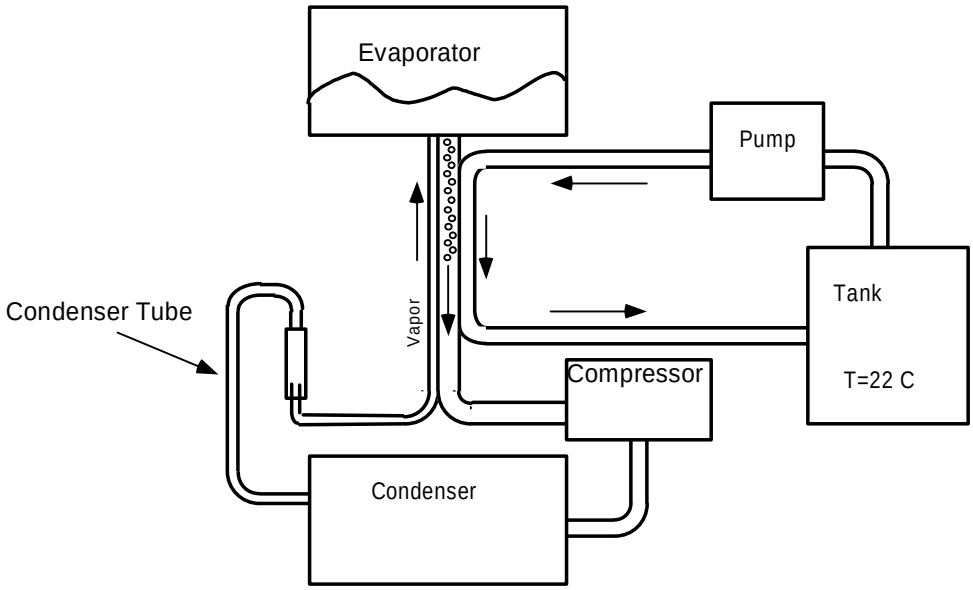

Figure 14 – Warming of Suction Line

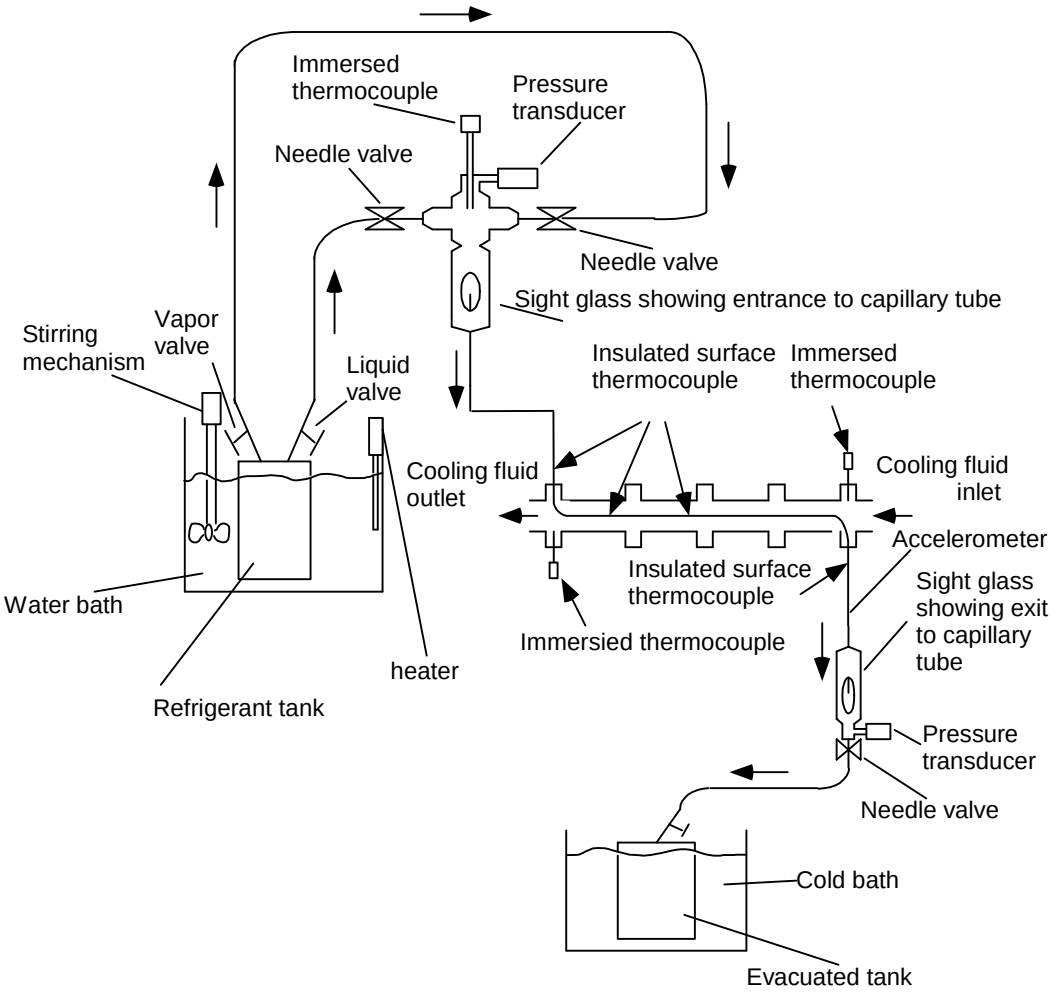

Figure 15 – Experimental Apparatus Schematic (0.91 mm capillary tube inner diameter, 2.23 mm capillary tube outer diameter, 15.9 mm coolant tube inner diameter, 1.27m capillary tube length from simulated filter dryer to heat exchanger inlet, 1.37m capillary tube length within counter flow heat exchanger, and 0.41m capillary tube length from heat exchanger outlet to capillary tube outlet)

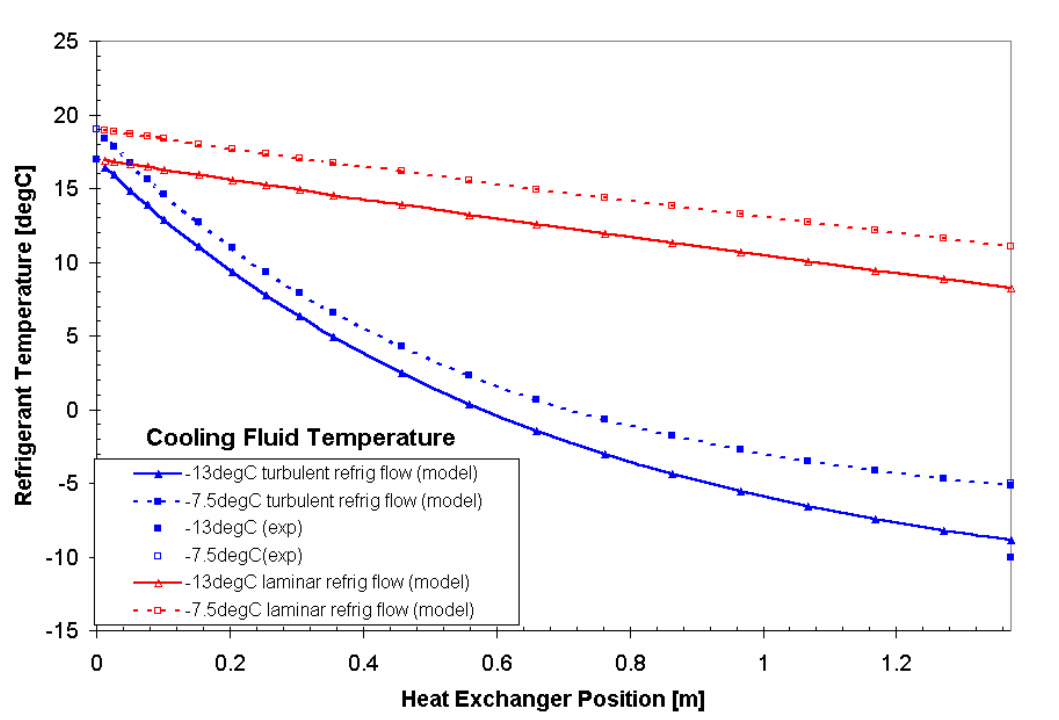

Figure 16 – Model Validation of Turbulent Flow Assumption at 689.5kPa

Table 1 – Household Refrigerator Instrumentation

Sensor	Location
Capillary Tube Exit Surface Thermocouple (T type)	Capillary tube/evaporator interface
Capillary Tube Inlet Surface Thermocouple (T type)	203 mm downstream of filter dryer
Suction Line Inlet Surface Thermocouple (T type)	Capillary tube/evaporator connection
Suction Line Exit Surface Thermocouple (T type)	304 mm upstream of compressor
Filter Dryer Top Immersed Thermocouple (T type)	Top of filter dryer filling port
Suction Line Pressure Transducer	Suction line/evaporator connection
Filter Dryer Top Pressure Transducer	Top of filter dryer filling port
Capillary Tube Exit Accelerometer	Capillary tube/evaporator interface